The Company of
Biologists

RESEARCH ARTICLE

Upstroke-based acceleration and head stabilization are the norm for the wing-propelled swimming of alcid seabirds

Anthony B. Lapsansky* and Bret W. Tobalske

ABSTRACT

Alcids, a family of seabirds including murres, guillemots and puffins, exhibit the greatest mass-specific dive depths and durations of any birds or mammals. These impressive diving capabilities have motivated numerous studies on the biomechanics of alcid swimming and diving, with one objective being to compare stroke–acceleration patterns of swimming alcids with those of penguins, where upstroke and downstroke are used for horizontal acceleration. Studies of free-ranging, descending alcids have found that alcids accelerate in the direction of travel during both their upstroke and downstroke, but only at depths <20 m, whereas studies of alcids swimming horizontally report upstroke-based acceleration to be rare (≤16% of upstrokes). We hypothesized that swimming trajectory, via its interaction with buoyancy, determines the magnitude of acceleration produced during the upstroke. Thus, we studied the stroke–acceleration relationships of five species of alcid swimming freely at the Alaska SeaLife Center using videography and kinematic analysis. Contrary to our prediction, we found that upstroke-based acceleration is very common (87% of upstrokes) during both descending and horizontal swimming. We reveal that head-damping – wherein an animal extends and retracts its head to offset periodic accelerations – is common in swimming alcids, underscoring the importance of head stabilization during avian locomotion.

KEY WORDS: Stroke acceleration patterns, Charadriiformes, Auk, Underwater locomotion, Diving

INTRODUCTION

When animals transition between air and water, they must cope with dramatic changes to their sensory perception, their respiration and the force regime to which they are subjected (Dial et al., 2015; Fish, 2016). Despite these challenges, the phylogeny of birds provides abundant examples of secondary adaption to life in water (Vermeij and Dudley, 2000). These species (e.g. ducks, cormorants, loons, puffins, penguins, etc.) can reach depths that rival those of much larger diving mammals (Ponganis, 2015).

Within birds, penguins (order Sphenisciformes, family Spheniscidae) appear to have been the most successful at re-invading the aquatic realm. The current records for dive depth and duration in birds are held by the ~25 kg emperor penguin (*Aptenodytes forsteri*) at 564 m and 27.6 min, respectively, with other penguin species not far behind (Ponganis, 2015). This aquatic accomplishment by penguins is often attributed to their loss of flight

Field Research Station at Fort Missoula, Division of Biological Sciences, University of Montana, 32 Campus Drive, Missoula, MT 59812, USA.

*Author for correspondence (anthony.lapsansky@umontana.edu)

A.B.L., 0000-0001-7530-7830; B.W.T., 0000-0002-5739-6099

(Elliott et al., 2013; Storer, 1960). The rationale behind this argument is that because air and water are drastically different (Denny, 1993), selection cannot optimize a species for movement in both fluids concurrently. In other words, abandoning flight has allowed penguins to better exploit the aquatic environment (Simpson, 1946).

However, the diving performance of alcids (order Charadriiformes), a family of seabirds closely related to gulls and terns, seems to contradict this notion. The alcid family contains 24 extant species including puffins, murres, guillemots and their relatives notable for their ability to 'fly' underwater as well as in the air. The current records for the depth and duration of a single dive by an alcid are 210 m and 224 s, respectively, held by the ~1 kg thick-billed murre (*Uria lomvia*), making this species, on a mass-specific basis, the deepest and longest-duration diver on Earth (Croll et al., 1992). When corrected for body size, alcids exhibit dive durations and depths far greater than penguins, despite remaining volant (Halsey et al., 2006; Watanuki and Burger, 1999).

The impressive diving capabilities of alcids have motivated multiple, independent studies on the biomechanics of alcid swimming and diving (Hamilton, 2006; Johansson and Aldrin, 2002; Kikuchi et al., 2015; Lovvorn et al., 2004; Watanuki and Sato, 2008; Watanuki et al., 2003, 2006), with one key focus being to compare stroke–acceleration patterns of swimming alcids with those of penguins.

The stroke–acceleration patterns of flying birds are well defined, both by empirical study and aerodynamic theory. To maintain speed, a flying bird must produce enough thrust to counteract drag. Flying alcids and similar species (e.g. ducks) are thought to produce this thrust primarily or entirely via the downstroke of their wing (Izraelevitz et al., 2018; Pennycuick, 1987; Rayner, 1988, 1995). The upstroke contributes to weight support, along with the downstroke, but is thought to produce only negligible thrust outside of slow flight (Crandell and Tobalske, 2015). Thus, owing to its stroke–acceleration pattern, an alcid maintaining speed during level, cruising flight should experience a horizontal deceleration during the upstroke followed by a horizontal acceleration of equal magnitude on the downstroke.

Though their style of swimming resembles the aerial flight of birds, swimming penguins deviate from this general stroke–acceleration pattern in ways hypothesized to increase to their efficiency (energy required to move at a given speed) (Clark and Bemis, 1979; Hui, 1988; Lovvorn, 2001; Watanuki et al., 2006). Swimming penguins accelerate forward during both downstroke and upstroke (Clark and Bemis, 1979; Hui, 1988; Watanuki et al., 2006). Perhaps owing to modifications of their flight apparatus only feasible through the loss of flight (Raikow et al., 1988), penguins produce significant amounts of thrust via their upstroke, as well as their downstroke, which is great enough to overcome the drag (and sometimes buoyancy) of their body. By accelerating during both halves of the stroke cycle, penguins minimize the magnitude of

accelerations needed to maintain speed (Watanuki et al., 2006). The alternative – large deceleration during the upstroke followed by compensatory acceleration during the downstroke – causes an animal to experience large deviations from its average velocity. This is especially true in water, where the drag is greatly increased relative to air (Denny, 1993). Because drag increases quadratically with velocity, and because it is energetically expensive to accelerate a body and its entrained fluid, an animal that moves at a more constant velocity spends less energy to move at the same average velocity (Daniel, 1984; Lovvorn, 2001; Vogel, 1994). Thus, by accelerating forward during the upstroke in addition to during the downstroke, penguins appear to have developed a highly efficient swimming strategy.

All alcids studied to date have shown at least some capacity to accelerate forward (hereafter, accelerate) during the upstroke when swimming, in addition to during the downstroke, but the conditions that determine the presence and frequency of upstroke-based acceleration remain unclear. Using the pattern of bubbles released by the plumage of a captive pigeon guillemot (*Cepphus columba*) as evidence, Rayner (1995) suggested that alcids had a hydrodynamically inactive aquatic upstroke that functioned exclusively to reset the wing for the next downstroke. Subsequent data collected via 3D videography of horizontally swimming alcids at relatively shallow depths found that the upstroke was capable of producing thrust, contrary to Rayner's assertion, but that this thrust rarely caused acceleration. Specifically, Johansson and Aldrin (2002) reported acceleration during 2 of 24 (8%) upstrokes by Atlantic puffins (*Fratercula arctica*) and Hamilton (2006) reported acceleration during 5 of 32 (16%) upstrokes by common murres (*Uria aalge*), suggesting that the force created by the upstroke of a swimming alcid is only rarely sufficient to overcome drag. In contrast, data collected via accelerometers on free-ranging alcids indicate that these animals regularly accelerate during the upstroke when descending, but that the magnitude of this acceleration decreases to below zero past depths of approximately 20 m (Lovvorn et al., 2004; Watanuki et al., 2003, 2006).

Previous authors have evoked the decrease in buoyancy with depth (as air in the lungs and plumage compress as described by Boyle's law) to explain the negative relationship between the magnitude of acceleration during the upstroke and depth (Lovvorn et al., 2004; Watanuki et al., 2003, 2006). However, if alcids accelerate during the upstroke when buoyancy is high, it is unclear why Johansson and Aldrin (2002) and Hamilton (2006) did not detect consistent upstroke-based acceleration in alcids swimming in shallow water.

We hypothesized that trajectory might determine the use of upstroke-based acceleration in swimming alcids via the relationship between trajectory and buoyancy. When descending in shallow water, work against buoyancy is a major contributor to the total work required to swim. In contrast, when swimming at depth and horizontally, little work must be done against buoyancy to maintain speed (Lovvorn, 2001), perhaps alleviating the need for upstroke-based acceleration. Thus, the interaction between trajectory and buoyancy may explain the decrease in upstroke-based acceleration with depth over the course of the same dive in descending alcids (Lovvorn et al., 2004; Watanuki and Sato, 2008; Watanuki et al., 2003, 2006) and the rarity of upstroke-based acceleration in horizontally swimming alcids (Hamilton, 2006; Johansson and Aldrin, 2002). To test this hypothesis, we studied the stroke–acceleration relationships of five species of alcids from three genera using videography and kinematic analysis. Our study subjects were captive birds swimming freely in an aquarium at the Alaska SeaLife Center in Seward, Alaska.

MATERIALS AND METHODS
Study area and animals
Study animals included common murres [*Uria aalge* (Pontoppidan 1763)], pigeon guillemots (*Cepphus columba* Pallas 1811), rhinoceros auklets [*Cerorhinca monocerata* (Pallas 1811)], horned puffins [*Fratercula corniculata* (Naumann 1821)] and tufted puffins [*Fratercula cirrhata* (Pallas 1769)]. This work was performed with permission from the Alaska SeaLife Center in Seward, Alaska, USA, from 23 to 31 June 2018 under the auspices of the University of Montana's Institutional Animal Care and Use Committee (AUP 004-19BTDBS-020419). The Alaska SeaLife Center is to home to an outdoor aviary exhibit with a large area for aerial flight (approximately 20 m wide, 20 m long and 8–10 m tall) over a 397,500 liter saltwater tank. The surface of the water measures approximately 10.5×11 m and is approximately 6.5 m deep at its deepest point. The southern edge of the tank is inset with a large glass viewing window approximately 3.5 m wide that extends from ∼2 m above the waterline to the floor of the tank. The glass of the viewing window varies from ∼6.5 to ∼25.0 cm thick from the waterline to the floor of the tank.

At the time of this study, the exhibit contained 12 horned puffins, 10 tufted puffins, four pigeon guillemots, six common murres and two rhinoceros auklets. Individuals of each species of alcid regularly swam past the viewing window, performing both horizontal and descending swimming bouts, either for transport around the exhibit or to retrieve food tossed in the water by aquarium staff. The birds swam on their own volition and selected their own swimming speeds and descent angles.

Videography
Videos were taken using a GoPro Hero6 Black (GoPro, Inc., San Mateo, CA, USA) at 119.88 frames s^{-1} and a shutter speed of 1/480 s in the 'Linear View' mode, which removes the 'fisheye' distortion common to action cameras (Tyson Hedrick, personal communication). The camera was positioned on a tripod and leveled using a bubble-type level embedded in the tripod. Because birds chose when and where to dive, swimming bouts were sampled opportunistically. The camera was triggered via a GoPro Smart Remote when A.B.L. noticed a bird about to initiate a dive or swim past the viewing window. The camera was positioned approximately 1 m below the waterline, thus all analyzed dives were between 0 and 3 m deep.

Kinematic and data analyses
Swimming bouts were selected for kinematic analysis based on whether birds appeared to swim at an approximately constant speed, parallel to the viewing window (perpendicular to the camera) as determined by A.B.L. We were stringent in this assessment, selecting less than 5% of all footage for analysis. Preference was given to videos taken on days with brighter natural light to facilitate the digitization process. We analyzed 41 swimming bouts totaling 166 downstrokes and 153 upstrokes (for condition- and species-specific values, see Table 1).

Although each bird in the tank had unique colored leg bands, we were unable to confidently identify individuals in video sequences. Thus, we considered each wingbeat as having been sampled from a greater population of wingbeats representing each species. Previous research on diving kinematics has indicated that this method provides a reasonably accurate kinematic description for a given species (Lovvorn et al., 1991). Given the number of individuals of each species in the tank and the number of swimming bouts we analyzed, it is unlikely that our data for any one species is based on fewer than two individuals (≤6.25%).

Table 1. Sample sizes for each alcid species and swimming trajectory

Species	Horizontal bouts	Descending bouts	Downstrokes during horizontal bouts	Upstrokes during horizontal bouts	Downstrokes during descending bouts	Upstrokes during descending bouts
Common murre	7	2	25	25	10	11
Horned puffin	6	3	25	23	10	8
Pigeon guillemot	5	3	27	25	8	8
Rhinoceros auklet	6	–	24	18	–	–
Tufted puffin	6	3	25	24	12	11

We performed kinematic analyses using MATLAB (2018a & b, MathWorks, Inc., Natick, MA, USA) using the DLTdv6 digitization tool described in Hedrick (2008) with additional analyses performed using MATLAB and IGOR Pro (v. 6.01, Wavemetrics, Inc., Beaverton, OR, USA). We assigned each swimming bout as being either horizontal (trajectory <5 deg from horizontal) or descending (>20 deg). We did not obtain video of rhinoceros auklets engaged in descending swimming.

We digitized the eye, the wrist and the tip of the tail in every frame of each video. To reduce digitizing error for the eye, we digitized the eye using three consecutively blind, replicate passes for horizontal bouts and averaged the three points at each frame. We only digitized the eye one time for descending bouts after realizing that birds were head-damping, wherein an animal extends and retracts the head to offset periodic accelerations and stabilize head position (Necker, 2007; Pete et al., 2015). An additional two points were digitized (at a single frame) corresponding to the waterline at opposite sides of the viewing window so that we could calculate the angle of descent. More than 43,000 points were hand-digitized for this study.

The x–y points determined via digitization were exported to MATLAB for analysis via a custom script. The script first computed the angle between the vector describing the true horizontal (i.e. the waterline) and the x-direction of the video. The script then rotated all digitized points about this angle, which was usually less than 1 deg, to account for small errors in the manual leveling of the camera setup. For descending bouts, the script then computed the angle between the vectors describing the bird's mean path and the vector corresponding to the waterline. The script then converted, via a 2D Euler-angle rotation matrix, the points from a global coordinate system to a local, bird-centered coordinate system in which the x- and y-axes were parallel and perpendicular to the bird's swimming direction, respectively. For horizontal bouts, we assumed that the x- and y-axes were reasonably aligned with the birds' cranial-caudal and dorsal-ventral axes and, therefore, did not transform the digitized points. Following transformation of the descending bouts, the MATLAB scripts were identical.

We used the body length of the bird in each frame, as determined by the distance between the eye and the tail in each frame, to convert the x–y points to a consistent coordinate system. This method of calibration accounts for variability in the distance between the camera and the bird as well as any distortion of the image that may have occurred as the light reflecting off the bird passed from water to glass to air before reaching the camera. Specifically, we computed the length of the body (in pixels) for each frame as the distance between the eye and the tail using the Pythagorean theorem. Visual inspection of these data revealed pronounced head movement (relative to the body) in sync with the wingbeat cycle (i.e. body length varied with position in the stroke cycle). Because of this observation, we smoothed the raw body-length data using the 'smoothingspline' method of fitting in MATLAB and a smoothing parameter of 1E-4 to account for the head movement of the bird (Curve Fitting ToolBox User's Guide, 2019;

https://www.mathworks.com/help/pdf_doc/curvefit/curvefit.pdf). The x–y points for each frame were then divided by the body length at that frame to convert the points' pixel units to units of body length. It should be noted that even if this calibration process was imperfect – for example, if the smoothing failed to remove the effects of head-damping completely – it would not alter our major conclusions about the hydrodynamic function of the upstroke. Upstroke with periods of acceleration would still have periods of acceleration, as body length was used simply to scale the data to units of species-specific body length. Only the magnitude of that acceleration could change.

We opted not to convert from body length units to SI units, as data on body length while swimming are available only for the common murre (within Hamilton, 2006). Because alcids flex their neck when diving, measurements taken from birds in the hand or from museum species are not accurate proxies for the body length a species adopts when swimming. Thus, we felt that using an estimate of body length for the other four species would add error to our results without improving our ability to test our hypothesis. However, we include rough estimates of body lengths during swimming for comparison: common murre, 0.36 m; horned puffin, 0.31 m; pigeon guillemot, 0.27 m; rhinocerous auklet, 0.30 m; tufted puffin, 0.35 m. We caution against using these values as true data points or in strict analyses. The conversion factor for the common murre comes from Hamilton (2006) and is based on two birds. Those for the tufted puffin, horned puffin and rhinoceros auklet (which are all, technically, puffins; Wilson and Manuwal, 1986) stem from the measured body length of a single Atlantic puffin (0.290±0.006 m), found by using ImageJ to compute the distance between 20 pairs of beak and tail points displayed in fig. 3B of Johansson and Aldrin (2002). Assuming geometric similarity between these four closely related species, we computed body length estimates in meters using mean masses from Dunning (2008). For the pigeon guillemot, we report a value measured on wild birds in the hand (we think) from Cody (1973). This value is almost certainly an overestimate and should be treated with caution. We encourage future studies to publish body lengths of animals during locomotion to facilitate research on animal locomotion under conditions in which calibration to metric units is infeasible (e.g. birds flying in the natural environment).

To account for digitization error, we smoothed the kinematic data using the same 'smoothingspline' method of fitting in MATLAB as above but using a smoothing parameter of 0.01 (Curve Fitting ToolBox User's Guide, 2019; https://www.mathworks.com/help/pdf_doc/curvefit/curvefit.pdf), based on Clifton and Biewener (2018) (Fig. 1). We computed instantaneous velocity (body lengths s^{-1}; hereafter BL s^{-1}) in the x-direction as the change in x-position between frames divided by the duration of the frame (1/119.88 s or 0.0083 s) for both eye and tail points (separately). We subsequently computed instantaneous acceleration (BL s^{-2}) as the change in velocity between frames divided by the duration of the frame. Because we digitized distal portions of the body rather than the center of mass, pitching motions of the body could impact our
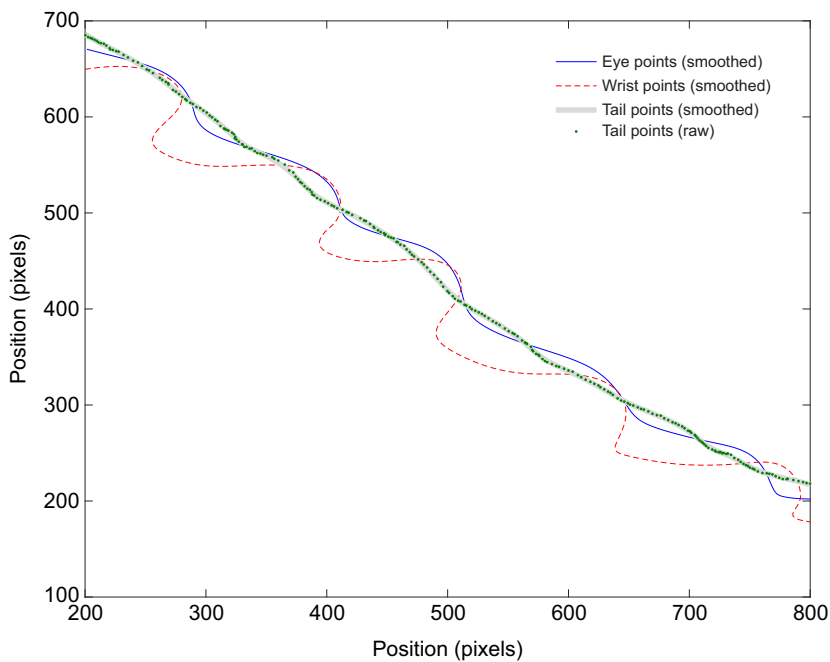
Fig. 1. Wing and body kinematics of a descending tufted puffin. Included are the raw, digitized tail points (green dots) and smoothed points corresponding to the tail, eye and wrist. Data from this bout are illustrated in Figs 2 and 3.

estimates of overall body acceleration. To resolve this potential issue, we first computed the pitch angle (rad) in each frame relative to the horizontal. This allowed us to remove the component of our velocity calculation that was due to pitching from the overall velocity calculation described above. Specifically, we assumed that the body pitched around a point midway between the eye and the tail, or about the approximate center of mass. Thus, the velocity due to body pitch was calculated as the change in x-oriented body length, where the x-oriented body length was computed as 0.5 times the body length times the cosine of the pitch angle. We removed this pitching velocity (BL s^{-1}) from the overall velocity of both the eye and the tail before computing acceleration. Because the change in pitch angle between adjacent frames was generally quite small relative to the change in body position, and because the pitch angles themselves were small relative to each bird's trajectory, pitching generally accounted for <5% of total acceleration. To this end, we

repeated our analyses while ignoring the effects of pitching and found no significant changes to our major results.

To differentiate between the upstroke and downstroke, we computed the elevation of the wrist (relative to the midline of the body defined as a line between the eye and tail). These data, along with the velocity and acceleration data, were then exported to IGOR Pro. We then manually picked the start and stop of each wing stroke, defined by the maximum and minimum elevation of the wrist, and used a custom macro to obtain the instantaneous velocity and acceleration data based on the tail and eye points between the two points in time.

Visual inspection of the body-length data revealed obvious head movement relative to the body in all five species (Fig. 2). For this reason, we present acceleration data based on the tail points, but for the sake of comparison with previous work (Hamilton, 2006; Johansson and Aldrin, 2002), we also used the eye points to compute the proportion of upstrokes with positive instantaneous acceleration.
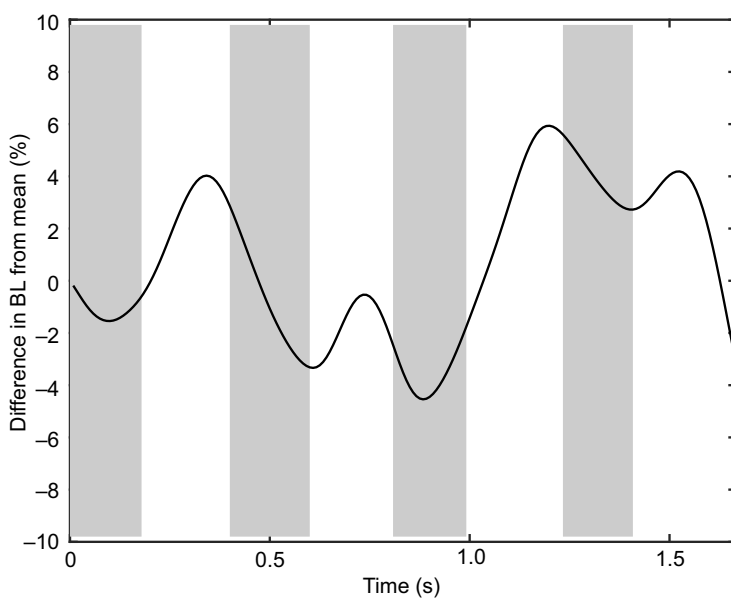
Fig. 2. Percent difference in body length (BL) relative to mean body length for a descending tufted puffin as a function of time (s). Gray background, downstroke; white background, upstroke, based on the position of the wrist. Body length is measured as the distance between the eye and the tail at each frame, after smoothing. These data were obtained from the sequence of wingbeats shown in Fig. 1.

We feel that the tail is a valid indicator of overall body motion in this study. Although the tail may be used for maneuvering in some species, we did not digitize bouts in which alcids changed direction or turned. In addition, the tail is folded when diving, and thus represents a fairly stiff offshoot of the body. Though it may have been worthwhile to digitize multiple points around the border of the body to estimate the location of the center of mass of each bird for each frame, the time required for such a process makes it unfeasible for a study with this large of a sample size. Further, automated tracking methods were unable to distinguish the bird from other objects in the tank, given the complex background.

To determine whether a given stroke resulted in acceleration, we used the 'findpeaks' function in MATLAB to locate the position and magnitude of the largest local maximum acceleration (hereafter, 'peak acceleration'), which typically occurred at around mid-stroke (Fig. 3). We chose this method over simply selecting the largest accelerations to avoid sampling momentary positive accelerations occurring at the stroke reversals and to better replicate the methods of past studies, which specifically refer to acceleration peaks (Hamilton, 2006; Watanuki et al., 2006).

The upstroke and downstroke of alcids contain highly negative and positive instantaneous accelerations that are variable in their timing between wingbeats. We found that because of this variability in timing, averaging the instantaneous acceleration across wing strokes leads to the deconstruction of the overall pattern (negative features overlap with positive features owing to slight variation in timing). Presumably for this reason, past studies have presented 'representative' acceleration profiles rather than average plots (Lovvorn et al., 2004; Watanuki et al., 2003, 2006). In addition to a representative plot, for both downstroke and upstroke we plot the average peak acceleration (i.e. the largest local maximum occurring during each half-stroke, as described above), average minimum acceleration, and average acceleration at the downstroke-to-upstroke transition, along with the standard error in mean and timing of said values, to illustrate the overall shape of the acceleration profiles for each species.

Statistics

Plots were made using MATLAB's basic plotting functions. To determine whether alcids in our study head-bobbed or head-damped,

we compared the coefficient of variation in velocity (calculated as the standard deviation in velocity divided by the mean velocity; hereafter, $CV_{velocity}$) for each complete wingbeat cycle based on either tail points or eye points. To test for a significant difference between these measures, we used a linear mixed-effects model (with random effects on the intercept for both species and bout) in MATLAB. Head-bobbing is exhibited by many bird species in walking and swimming and occurs when a bird alternates between a globally fixed head position and a thrusting head movement in sync with the stroke cycle (Clifton and Biewener, 2018; Necker, 2007). Head-damping occurs when a bird uses relative head movement to smooth or damp the acceleration patterns of the body, thereby creating a more stable visual field. If birds head-bobbed, then we would expect higher $CV_{velocity}$ values owing to the alternation between hold and thrust phases of the head, whereas head-damping would result in lower $CV_{velocity}$ values. For values of maximum upstroke and downstroke, standard deviations were computed as the square root of the summed squared-errors for maximum upstroke and downstroke. We report means±s.e.m.

RESULTS

Stroke–acceleration pattern

On average, alcids accelerated during the downstroke and decelerated during the upstroke in both level and descending bouts (Table 2). However, 100 of 115 (87%) upstrokes during horizontal bouts and 33 of 38 (87%) upstrokes during descending bouts produced peak accelerations greater than zero (Table 2). In other words, alcids experienced moments of acceleration during the majority of upstrokes. The general stroke-acceleration pattern as a function of time was M-shaped across all five species, with minima near the stroke reversals and peaks at about mid-stroke (Figs 4 and 5). The relative height of mean peak upstroke-acceleration to mean peak downstroke-acceleration ranged from 0.23±0.28 BL s^{-2} in the pigeon guillemot to 0.61±0.22 BL s^{-2} in the tufted puffin for horizontal swimming, and from 0.06±0.50 in the horned puffin to 0.89± 0.35 BL s^{-2} in the pigeon guillemot for descending swimming (Figs 4 and 5, Table 2). The timing of peak acceleration during the downstroke was much more consistent than that during the upstroke, as illustrated by the width of the error bars in Figs 4 and 5. The peak
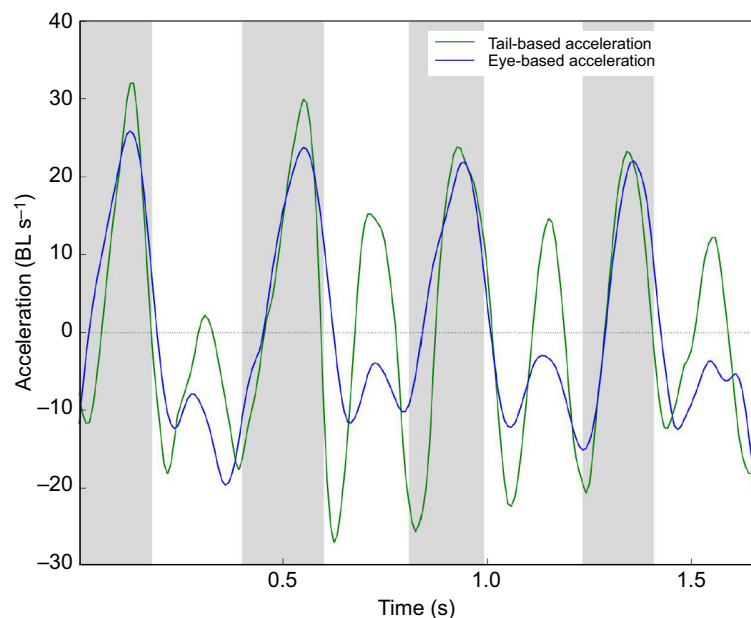
Fig. 3. Acceleration pattern (BL s^{-2}) of a descending tufted puffin, based on both head and tail points, versus time (s). Gray background, downstroke; white background, upstroke, based on the position of the wrist. These data are taken from the sequence of wingbeats shown in Fig. 1.

Table 2. Stroke–acceleration patterns for five species of alcid engaged in descending and horizontal swimming

	Common murre	Horned puffin	Pigeon guillemot	Rhinoceros auklet	Tufted puffin
Horizontal					
Mean downstroke acceleration (BL s^{-2})	6.32±1.20	8.64±0.67	3.98±0.89	7.88±1.89	4.03±0.75
Mean upstroke acceleration (BL s^{-2})	−2.44±0.50	−4.13±0.79	−3.56±0.65	−4.24±1.48	−0.923±0.56
Peak downstroke acceleration (BL s^{-2})	15.46±1.57	24.99±0.94	15.23±1.21	23.41±2.25	16.89±2.16
Peak upstroke acceleration (BL s^{-2})	6.07±0.73	9.04±1.82	3.57±0.97	8.68±1.95	10.23±1.88
Min. downstroke acceleration (BL s^{-2})	−5.29±0.98	−11.46±1.83	−8.73±1.00	−11.54±2.26	−8.58±2.18
Min. upstroke acceleration (BL s^{-2})	−11.51±1.17	−19.19±1.92	−13.05±1.14	−19.61±3.03	−10.93±1.65
Upstroke peak/downstroke peak	0.39±0.16	0.36±0.20	0.23±0.28	0.37±0.24	0.61±0.22
Prop. downstrokes with peak acceleration>0	24/25	25/25	27/27	23/24	25/25
Prop. upstrokes with peak acceleration>0	22/25	19/23	19/25	17/18	23/24
Prop. upstrokes with peak acceleration>0, based on head points	11/25	9/23	8/25	6/18	18/24
Descent					
Mean downstroke acceleration (BL s^{-2})	1.84±0.88	9.65±1.41	2.34±2.83		6.32±0.89
Mean upstroke acceleration (BL s^{-2})	−1.60±0.67	−5.18±0.55	−0.834±3.52		−3.92±0.74
Peak downstroke acceleration (BL s^{-2})	13.38±1.04	27.45±2.25	17.11±2.55		26.78±1.17
Peak upstroke acceleration (BL s^{-2})	6.35±1.11	1.53±0.76	15.22±4.77		7.77±1.08
Min. downstroke acceleration (BL s^{-2})	−11.38±1.86	−10.62±1.90	−19.88±2.21		−14.30±1.60
Min. upstroke acceleration (BL s^{-2})	−11.79±1.37	−16.52±1.23	−17.03±2.37		−16.84±1.46
Upstroke peak/downstroke peak	0.47±0.19	0.06±0.50	0.89±0.35		0.29±0.15
Prop. downstrokes with peak acceleration>0	10/10	10/10	8/8		12/12
Prop. upstrokes with peak acceleration>0	9/11	6/8	7/8		11/11
Prop. upstrokes with peak acceleration>0, based on head points	10/11	2/8	5/8		3/11

All data are based on tail points unless otherwise specified.
Data are presented as averages of the mean, peak and minimum accelerations, in terms of body lengths s^{-2} (BL s^{-2}) from all half-strokes±s.e.m.

downstroke-acceleration tended to be larger, and the peak upstroke-acceleration tended to be smaller, for descending swimming relative to horizontal swimming, though the general stroke–acceleration pattern is consistent under both conditions (Figs 4 and 5).

Head-damping and impacts on perceived stroke-acceleration patterns

Alcids of all five species exhibited head movement relative to the movement of their bodies in sync with their stroke cycle (Fig. 2).

We were interested in whether this head movement reflected 'head-bobbing' or 'head-damping' (Necker, 2007; Pete et al., 2015). To test between these two options, we compared $CV_{velocity}$ when computed based on the eye versus that computed based on the tail for all complete wingbeats. The mean $CV_{velocity}$ based on the eye was significantly lower than that based on the tail ($P=0.015$), thus indicating head-damping.

In comparing stroke–acceleration patterns based on the tail- versus eye-position, head-damping had a clear effect on whether we detected
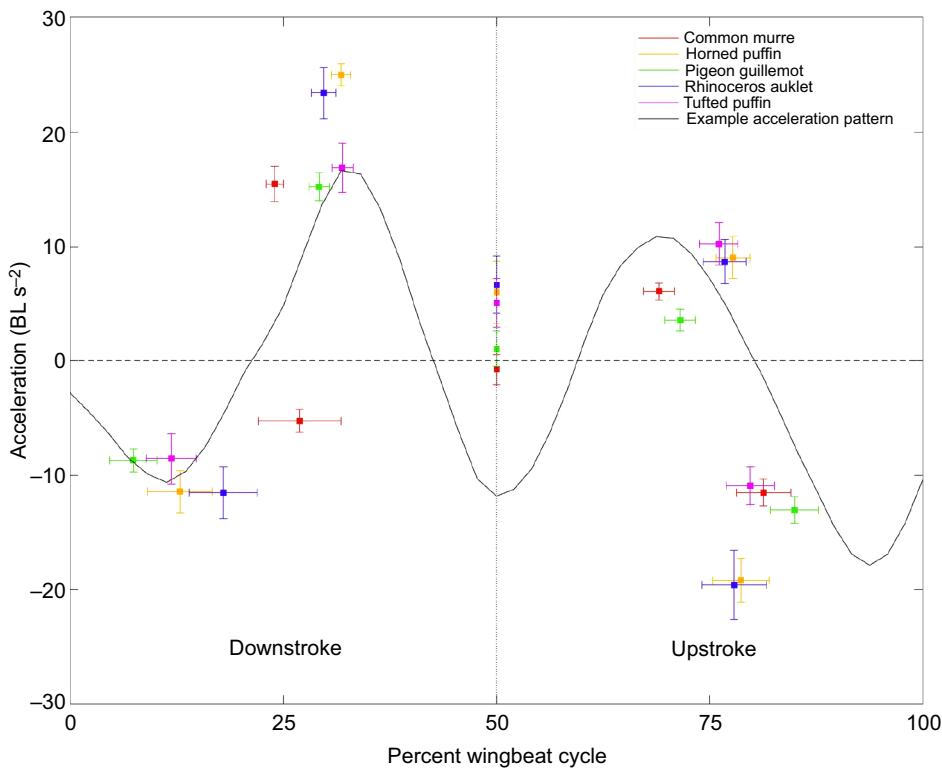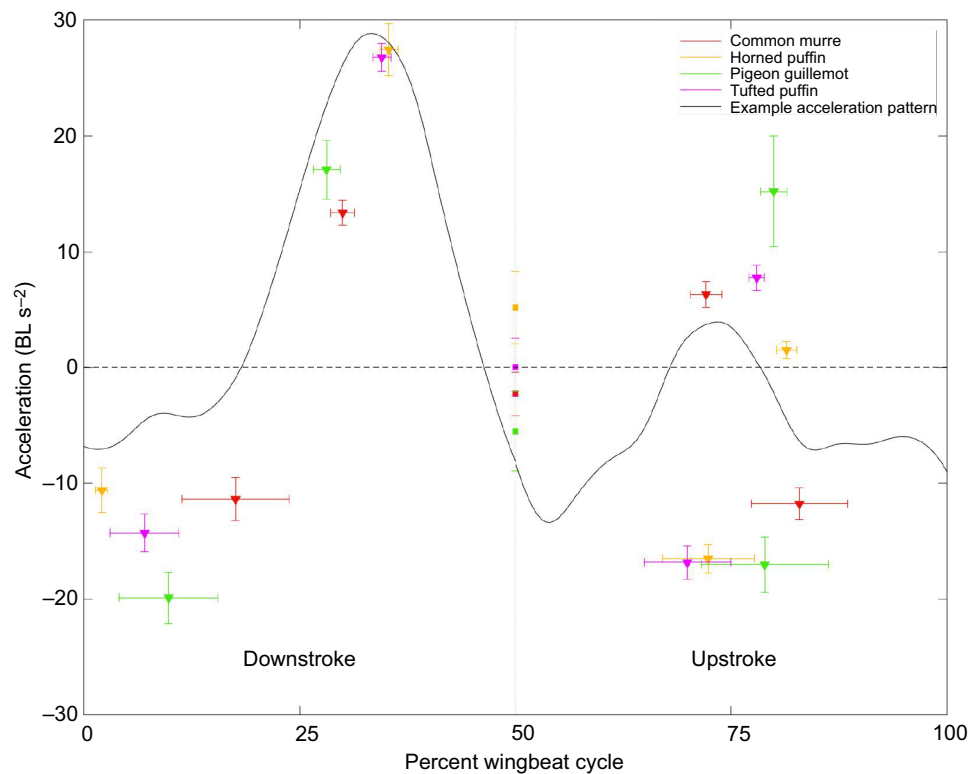

Fig. 4. Acceleration (BL s^{-2}) patterns of five species of alcid in horizontal swimming, based on tail points. Points correspond to the average of all peak and minimum accelerations from each of the sampled half-strokes, along with the average acceleration at the downstroke–upstroke transition. Vertical error bars are the standard error in the magnitude of each point and horizontal error bars are the standard error in the timing of when the peak or minimum acceleration occurred in a given half-stroke. See Table 1 for sample sizes.

Fig. 5. Acceleration (BL s⁻²) patterns of four species of alcid in descending swimming, based on tail points. Points correspond to the average of all peak and minimum accelerations from each of the sampled half-strokes, along with the average acceleration at the downstroke–upstroke transition. Vertical error bars are the standard error in the magnitude of each point and horizontal error bars are the standard error in the timing of when the peak or minimum acceleration occurred in a given half-stroke. See Table 1 for sample sizes.

acceleration on the upstroke. When acceleration was calculated based on the position of the tail, 100 of 115 (87%) horizontal upstrokes and 31 of 38 (87%) descending upstrokes had peak accelerations >0 BL s⁻² (Table 2). In contrast, when acceleration was calculated based on the position of the eye, 52 of 115 (45%) horizontal upstrokes and 20 of 38 (53%) of descending upstrokes had peak accelerations >0 BL s⁻² (Table 2). For example, in a single sequence of wingbeats from a descending tufted puffin, 4 of 4 upstrokes showed peak accelerations >0 BL s⁻² when computed based on tail points, whereas 0 of 4 showed peak accelerations >0 BL s⁻² when computed based on head points (Fig. 3).

DISCUSSION
Our results revise understanding of the stroke–acceleration patterns of swimming alcids and offer new insights into the ubiquity of visual stabilization in avian locomotion.

Contrary to our hypothesis that the presence of upstroke-based acceleration was determined by swimming trajectory, we found that the upstroke consistently resulted in acceleration of the body (133 of 153 upstrokes, 87%) in both horizontal and descending swimming, with peak accelerations ranging from 23 to 61% and 6 to 89% of that produced during the downstroke in horizontal and descending swimming, respectively (Table 2, Figs 4 and 5). This result is contrary to those of two previous studies of horizontal swimming in alcids, which found peak accelerations significantly greater than zero in only 2 of 24 (8%) upstrokes of Atlantic puffins (Johansson and Aldrin, 2002) and 5 of 32 (16%) upstrokes of common murres (Hamilton, 2006). Our unique result is likely due to previous kinematic studies including either the position of the head, or regions of the body that are distorted by head movement, in their computations of body acceleration. Our study indicates that the position of the head is not a reliable indicator of overall body position for swimming alcids (Fig. 2). Had we used the head to compute body accelerations, we would have obtained results more

consistent with those of past studies (see data within Table 2, 72 of 153 upstrokes producing acceleration, 47%).

Our study also differs from those of Johansson and Aldrin (2002) and Hamilton (2006) in other, contrasting ways. Thanks to recent advancements in high-speed camera technology, we were able to record birds swimming in a much larger volume of water (397,000 liters) than in past kinematic studies. Johansson and Aldrin (2002) and Hamilton (2006) were limited to the use of small tanks to meet the lighting requirements of early-2000s high-speed cameras. Johansson and Aldrin (2002) studied Atlantic puffins in a tank measuring 5×1×1 m and Hamilton (2006) studied common murres in a water tunnel with a working section measuring 4.4×0.8×0.6 m. These dimensions may have restricted the range of motion of the animals. In addition, Johansson and Aldrin (2002) studied wild-caught birds, whereas we and Hamilton (2006) studied captive-raised birds. The lack of opportunities to engage in sustained flight in captive birds may affect the flight muscles in ways that affect swimming performance. Further, Johansson and Aldrin (2002) filmed birds as they fled from an approaching researcher, and Hamilton (2006) measured accelerations at series of fixed swimming velocities, whereas birds in our study were free to choose when, where and how fast to swim.

Nonetheless, birds in our study were confined to swim at rather shallow depths (<6.5 m), and our sampled bouts of swimming were at depths ≤3 m. This has implications for interpreting our results in relation to diving in the wild because of the likely effects of buoyancy. Penguins prepare extensively for dives by increasing their breathing rate (Wilson, 2003) and appear to modulate their lung volume based on the depth of the upcoming dive (Sato et al., 2002, 2011). We know of no study in alcids on the relationship between lung volume and dive depth, but, similar to Wilson (2003), we did observe pre-dive panting in rhinoceros auklets, tufted puffins and horned puffins. In addition, common murres opened their beak to a wide angle just before diving. If alcids control the volume of air

in their lungs based on the depth of the upcoming dive like penguins, then alcids in our study were likely less buoyant than free-ranging birds. Thus, the magnitude of acceleration during the upstroke we measured may be larger than these species experience when diving to greater depths.

The pitching motions alcids exhibit when swimming may have also disguised the stroke–acceleration patterns of animals in previous kinematic studies; however, our data suggest that this is unlikely. We accounted for the impacts of pitching in our acceleration calculations, but had we not, our results for the relative frequency of upstroke-based acceleration would have been similar. When the effects of pitching were ignored, and acceleration was computed based on the position of the tail, alcids appeared to accelerate on 104 of 115 (90%) upstrokes during horizontal bouts and 33 of 38 (87%) upstrokes during descending bouts. When the effects of pitching were ignored, and acceleration was computed based on the position of the eye, alcids appeared to accelerate on 57 of 115 (50%) upstrokes during horizontal bouts and 21 of 38 (55%) upstrokes during descending bouts. These results largely mirror our pitch-controlled results, suggesting that head-damping is the primary reason that previous kinematic studies failed to detect consistent upstroke-based acceleration in swimming alcids (Hamilton, 2006; Johansson and Aldrin, 2002). The body angle of swimming alcids is generally quite close to their angle of descent (generally <10 deg difference), limiting the impact of pitching on acceleration calculations.

Studies that have used accelerometers to track the stroke–acceleration patterns of free-ranging alcids have found that alcids accelerate during the upstroke only in shallow water (0–20 m) (Lovvorn et al., 2004; Watanuki et al., 2003, 2006). These authors have hypothesized that the decrease in buoyancy with depth, which occurs as air volumes in the bird's respiratory system and plumage compress, is responsible for the decrease in peak upstroke-based acceleration. Our results indicate that this phenomenon is not driven by the trajectory of the animal (Lovvorn et al., 2004; Watanuki and Sato, 2008; Watanuki et al., 2006).

Interestingly, alcids decrease upstroke-based acceleration with depth while maintaining relatively consistent downstroke kinematics (Watanuki and Sato, 2008; Watanuki et al., 2006). As an explanation for this behavior, Watanuki and Sato (2008) and others suggest that alcids vary upstroke kinematics to control their speed in response to changing buoyancy. In other words, as buoyancy decreases with depth, alcids reduce the thrust produced by their upstroke rather than increase their speed, perhaps to minimize drag costs (Watanuki et al., 2003). This explanation fits with evidence from Lovvorn et al. (1999), who found that many diving birds have characteristic speeds with minimum coefficients of drag. However, given that a less-pulsatile acceleration profile should decease the cost of swimming at a given speed (Lovvorn, 2001; Vogel, 1994), it is unclear why birds would decrease the thrust produced by the upstroke alone, rather than vary the kinematics of both the downstroke and upstroke in conjunction to control their speed.

We offer a potential explanation for why alcids rely on the upstroke to regulate swimming speed based on the volume of the muscle powering the stroke and the characteristic efficiency of muscle fibers. This explanation assumes the contractile dynamics of the major wing muscles (pectoralis and supracoracoideus) may be inferred from wing motion. Watanuki and Sato (2008) found that upstroke duration, but not downstroke duration, varies significantly with depth. Assuming that stroke amplitude does not vary concurrently with depth, the results of Watanuki and Sato (2008) indicate that alcids alter upstroke velocity, and, by relation, strain rate of the

supracoracoideus muscle, to alter the thrust produced by their upstroke. Muscle fibers of a given fiber type are most efficient over a narrow range of strain rates (Goldspink, 1977; He et al., 2000; Reggiani et al., 1997). Thus, varying strain rate with depth, while likely minimizing drag costs (Lovvorn et al., 1999), probably reduces the average contractile efficiency of supracoracoideus contraction. However, the cost of contracting fibers in the supracoracoideus at an inefficient strain rate may be relatively small, as the supracoracoideus is small relative to the pectoralis (Kovacs and Meyers, 2000). The total energetic cost of a contraction at an inefficient strain rate is equal to the cost per muscle fiber times the number of fibers involved. Thus, it may require less energy to contract the supracoracoideus at highly inefficient rates of strain, given its small volume, rather than vary strain rate to a lesser extent in both the supracoracoideus and the larger pectoralis. In other words, alcids may minimize the energetic costs of swimming by maintaining downstroke kinematics across depths at values that maximize the contractile efficiency of the pectoralis – varying upstroke kinematics instead – despite the acceleration-related costs.

Alcids in the present study appeared to utilized head-damping to smooth instantaneous accelerations while swimming, rather than exhibiting the more traditional pattern of head-bobbing observed in foot-propelled swimming loons (Clifton and Biewener, 2018) and grebes (Gunji et al., 2013). Head-bobbing is characterized by alternating between the hold and thrust phases of the head, each of which may have a different function. According to Necker (2007), the hold phase likely aids in object detection, whereas the thrust phase may improve a bird's ability to determine depth based on the rate of optic flow, defined as the rate that the image of the world moves across the retina (Martin, 2017). Head-damping has been more commonly documented in flying birds and is a critical aspect of flight, wherein it functions to stabilize optic flow (Dakin et al., 2016; Goller and Altshuler, 2014; Pete et al., 2015; Ros and Biewener, 2016, 2017; Walsh et al., 2013). Head-damping in swimming alcids may perform a function similar to its role in aerial flight. Alternatively, owing to the kinematic similarities between aerial flight and wing-propelled swimming in these species, alcids may perform head-damping involuntarily because of to rigid connections between motor neurons and vestibular/ocular pathways in the brain. Moreover, excluding pigeon guillemots, alcids have much shorter necks than either loons or grebes, and head-bobbing may be ineffective for species lacking long necks. Exploring the head motion of diving alcids may reveal novel insights into the general functioning of optic flow in avian locomotion, and thus merits further study.

Based on the pattern of bubbles released from a swimming pigeon guillemot, Rayner (1995) predicted that the upstroke of all swimming alcids was inactive. Although studies of other alcid species have since disproved this position, it has remained possible that Rayner (1995) was correct with regards to pigeon guillemots, which are morphologically and ecologically distinct from other alcids (Ashmole, 1971). Relative to other alcids, pigeon guillemots are highly maneuverable in slow flight (A.B.L., personal observation) and forage in shallow water (Clowater and Burger, 1994). Our results indicate that the wing-propelled swimming of pigeon guillemots is not distinct from that of other alcids. Instead, as pointed out by Johansson and Aldrin (2002), Rayner (1995) may not have observed vorticity produced by the upstroke, which would indicate force production, because the force of the water pressing on the upper surface of the wing during the upstroke prevented the release of bubbles from the feathers.

Penguins have been shown to experience accelerations of near-equal magnitude during both downstroke and upstroke (Clark and

Bemis, 1979; Hui, 1988; Watanuki et al., 2006). This information has been used as evidence that penguins are supremely adapted to swimming and, thus, more efficient underwater than alcids (Lovvorn et al., 2004; Rayner, 1995), which produce more unequal forces owing, potentially, to the trade-offs between aerial and aquatic performance. However, the fact that alcids have longer mass-specific dive durations than penguins (Halsey et al., 2006; Watanuki and Burger, 1999), and therefore seem to consume their oxygen supply more efficiently than penguins, calls into question this assumption. In line with this logic, we found that alcids experience upstroke-based accelerations ranging from 6 to 89% and 23 to 61% of that produced by downstroke in descending and horizontal swimming, respectively. In comparison, Watanuki et al. (2006) reports a downstroke-to-upstroke acceleration ratio for descending little penguins (*Eudyptula minor*) of approximately 74% at 2 m, while Hui (1988) reports a downstroke-to-upstroke acceleration ratio of 58% for Humboldt penguins (*Spheniscus humboldti*) swimming horizontally in shallow water. Thus, alcids produce thrust on both halves of their stroke cycle – enough thrust to cause acceleration during both half-strokes – and the available information indicates that the distribution of force production between upstroke and downstroke in alcids is only slight less even than that in penguins, at least in shallow water.

An additional factor in determining the efficiency of swimming is the hydrodynamic method of thrust production. Penguins produce force via lift-based hydrodynamic mechanisms on both the upstroke and downstroke thanks to the symmetric foil shape of their wings (Bannasch, 1995; Hui, 1988). At high speeds, lift-based propulsion is more efficient, in terms of the energy required to produce a given net thrust, than drag-based propulsion from both theoretical (Daniel and Webb, 1987; Jackson et al., 1992) and empirical perspectives (Baudinette and Gill, 1985; Fish, 1996; Richman and Lovvorn, 2008; Schmid et al., 1995; Vogel, 1994; Williams, 1999). If we assume that drag-based propulsion is synonymous with 'rowing' and lift-based propulsion with 'flapping' (Walker and Westneat, 2002), which is a coarse but reasonable approximation for the wing-propelled locomotion of diving birds (but see Johansson and Lindhe Norberg, 2000; Johansson and Lindhe Norberg, 2001; Johansson and Norberg, 2003), then lift-based propulsion is more efficient at all speeds (Walker and Westneat, 2000). By this logic, penguins have been considered especially efficient swimmers. However, our data present some evidence that the aquatic upstroke-thrust of alcids is also lift-based.

During the upstroke of alcids in our study, the wing appears to move forward (in addition to upward) relative to the body of the animal. Because the animal itself is moving forward, the wing moves forward relative to the water, as well (Fig. 1). If the upstroke were to produce force via drag, then it would have to move backward relative to the fluid to produce thrust. Thus, the upstroke of a swimming alcid appears to produce a lift force directed forward and downward – much like the upstroke of a penguin. Johansson (2003) reached a similar conclusion based on data from Atlantic puffins. Similarly, the alcid downstroke moves downward and slightly forward relative to the water (Fig. 1), suggesting that alcids produce lift forces for propulsion during both half-strokes (Johansson and Aldrin, 2002). However, because rowing kinematics are capable of producing larger forces at slow speeds (Walker and Westneat, 2000), alcids may utilize a more drag-based downstroke at slow speeds (to accelerate or counter large buoyant forces) and shift toward a more lift-based downstroke at high speeds. Further research is necessary to elucidate the exact hydrodynamic mechanisms by which alcids produce force in water, especially if we

wish to build bioinspired robots based on these animals (Lock et al., 2010, 2012, 2013).

Conclusions
Our study of five species from three genera confirms that alcids routinely accelerate during both the downstroke and upstroke in both horizontal and descending swimming at shallow depths. We found that the head is not a reliable indicator of body acceleration in swimming alcids because of head-damping, offering a potential explanation for the rarity upstroke-based acceleration detected in past studies of horizontally swimming alcids. Future studies should track the tail or, ideally, the center of mass of diving birds to eliminate the effects of relative head movement on force calculations. The use of head-damping reveals the ubiquity of the need for head stabilization during avian wing-propelled locomotion.

References
Ashmole, P. N. (1971). Sea bird ecology and the marine environment. *Avian Biol.* **2**, 223-286.
Bannasch, R. (1995). Hydrodynamics of penguins – an experimental approach. In *The Penguins: Ecology and Management* (ed. P. Dann, I. Normann and P. Reilly), pp. 141-176. Melbourne: Surrey Beatty & Sons.
Baudinette, R. V. and Gill, P. (1985). The energetics of "flying" and "paddling" in water: locomotion in penguins and ducks. *J. Comp. Physiol. B* **155**, 373-380. doi:10.1007/BF00687481
Clark, B. D. and Bemis, W. (1979). Kinematics of swimming of penguins at the Detroit Zoo. *J. Zool.* **188**, 411-428. doi:10.1111/j.1469-7998.1979.tb03424.x
Clifton, G. T. and Biewener, A. A. (2018). Foot-propelled swimming kinematics and turning strategies in common loons. *J. Exp. Biol.* 221, jeb168831. doi:10.1242/jeb.168831
Clowater, J. S. and Burger, A. E. (1994). The diving behaviour of pigeon guillemots (*Cepphus columba*) off southern Vancouver Island. *Can. J. Zool.* **72**, 863-872. doi:10.1139/z94-117
Cody, M. L. (1973). Coexistence, Coevolution and Convergent Evolution in Seabird Communities. *Ecology* **54**, 31-44. (doi:10.2307/1934372)
Crandell, K. E. and Tobalske, B. W. (2015). Kinematics and aerodynamics of avian upstrokes during slow flight. *J. Exp. Biol.* **218**, 2518-2527. doi:10.1242/jeb.116228
Croll, D. A., Gaston, A. J., Burger, A. E., Konnoff, D. and Gaston, A. J. (1992). Foraging behavior and physiological adaptation for diving in thick-billed murres. *Ecology* **73**, 344-356. doi:10.2307/1938746
Dakin, R., Fellows, T. K. and Altshuler, D. L. (2016). Visual guidance of forward flight in hummingbirds reveals control based on image features instead of pattern velocity. *Proc. Natl. Acad. Sci. USA* **113**, 8849-8854. doi:10.1073/pnas.1603221113
Daniel, T. L. (1984). Unsteady aspects of aquatic locomotion. *Am. Zool.* **24**, 121-134. doi:10.1093/icb/24.1.121
Daniel, T. L. and Webb, P. W. (1987). Physical determinants of locomotion. *Comp. Physiol. Life Water L.* 343-369.
Denny, M. W. (1993). *Air and Water: The Biology and Physics of Life's Media.* Princeton University Press.
Dial, K. P., Shubin, N. and Brainerd, E. (2015). *Great Transformations in Vertebrate Evolution.* The University of Chicago Press.

Dunning, J. B. (2008). *CRC Handbook of Avian Body Masses*. Second Edi. Boca Raton, London & New York: CRC Press.

Elliott, K. H., Ricklefs, R. E., Gaston, A. J., Hatch, S. A., Speakman, J. R. and Davoren, G. K. (2013). High flight costs, but low dive costs, in auks support the biomechanical hypothesis for flightlessness in penguins. *Proc. Natl. Acad. Sci. USA* **110**, 9380-9384. doi:10.1073/pnas.1304838110

Fish, F. E. (1996). Transitions from drag-based to lift-based propulsion in mammalian swimming. *Am. Zool.* **36**, 628-641. doi:10.1093/icb/36.6.628

Fish, F. E. (2016). Secondary evolution of aquatic propulsion in higher vertebrates: validation and prospect. *Integr. Comp. Biol.* **56**, icw123. doi:10.1093/icb/icw123

Goldspink, G. (1977). Mechanics and energetics of muscle in animals of different sizes, with particular reference to the muscle fibre composition of vertebrate muscle. In *Scale Effects in Animal Locomotion* (ed. T. J. Pedly), pp. 27-55. Academic Press.

Goller, B. and Altshuler, D. L. (2014). Hummingbirds control hovering flight by stabilizing visual motion. *Proc. Natl. Acad. Sci. USA* **111**, 18375-18380. doi:10. 1073/pnas.1415975111

Gunji, M., Fujita, M. and Higuchi, H. (2013). Function of head-bobbing behavior in diving little grebes. *J. Comp. Physiol. A* **199**, 703-709. doi:10.1007/s00359-013-0828-4

Halsey, L. G., Butler, P. J. and Blackburn, T. M. (2006). A phylogenetic analysis of the allometry of diving. *Am. Nat.* **167**, 276-287. doi:10.1086/499439

Hamilton, J. L. (2006). Alcid swimming: kinematics, muscle activity patterns and pelagic diving behavior. *PhD thesis, Brown University*.

He, Z.-H., Bottinelli, R., Pellegrino, M. A., Ferenczi, M. A. and Reggiani, C. (2000). ATP consumption and efficiency of human single muscle fibers with different myosin isoform composition. *Biophys. J.* **79**, 945-961. doi:10.1016/S0006-3495(00)76349-1

Hedrick, T. L. (2008). Software techniques for two- and three-dimensional kinematic measurements of biological and biomimetic systems. *Bioinspir. Biomim.* **3**, 034001. doi:10.1088/1748-3182/3/3/034001

Hui, C. (1988). Penguin swimming. I. Hydrodynamics. *Physiol. Zool.* **61**, 333-343. doi:10.1086/physzool.61.4.30161251

Izraelevitz, J. S., Kotidis, M. and Triantafyllou, M. S. (2018). Optimized kinematics enable both aerial and aquatic propulsion from a single three-dimensional flapping wing. *Phys. Rev. Fluids* **7**, 1-25. doi:10.1103/PhysRevFluids.3.073102

Jackson, P. S., Locke, N. and Brown, P. (1992). The hydrodynamics of paddle propulsion. *11th Aust. Fluid Mech. Conf.* 1197-1200. https://people.eng.unimelb. edu.au/imarusic/proceedings/11%20AFMC%20TOC.htm.

Johansson, L. C. (2003). Indirect estimates of wing-propulsion forces in horizontally diving Atlantic puffins (Fratercula arctica L.). *Can. J. Zool.* **81**, 816-822. doi:10. 1139/z03-058

Johansson, L. C. and Aldrin, B. S. W. (2002). Kinematics of diving Atlantic puffins (Fratercula arctica L.): evidence for an active upstroke. *J. Exp. Biol.* **205**, 371-378.

Johansson, L. C. and Lindhe Norberg, U. M. (2000). Asymmetric toes aid underwater swimming. *Nature* **407**, 582-583. doi:10.1038/35036689

Johansson, L. C. and Lindhe Norberg, U. M. (2001). Lift-based paddling in diving grebe. *J. Exp. Biol.* **204**, 1687-1696.

Johansson, L. C. and Norberg, R. A. Å. (2003). Delta-wing function of webbed feet gives hydrodynamic lift for swimming propulsion in birds. *Nature* **424**, 65-68. doi:10.1038/nature01695

Kikuchi, D. M., Watanuki, Y., Sato, N., Hoshina, K., Takahashi, A. and Watanabe, Y. Y. (2015). Strouhal number for flying and swimming in rhinoceros auklets *Cerorhinca monocerata*. *J. Avian Biol.* **46**, 406-411. doi:10.1111/jav.00642

Kovacs, C. E. and Meyers, R. A. (2000). Anatomy and histochemistry of flight muscles in a wing-propelled diving bird, the Atlantic puffin, Fratercula arctica. *J. Morphol.* **244**, 109-125. doi:10.1002/(SICI)1097-4687(200005)244:2<109:: AID-JMOR2>3.0.CO;2-0

Lock, R. J., Vaidyanathan, R., Burgess, S. C. and Loveless, J. (2010). Development of a biologically inspired multi-modal wing model for aerial-aquatic robotic vehicles through empirical and numerical modelling of the common guillemot, Uria aalge. *Bioinspir. Biomim.* **5**, 1-15. doi:10.1088/1748-3182/5/4/046001

Lock, R. J., Vaidyanathan, R. and Burgess, S. C. (2012). Design and experimental verification of a biologically inspired multi-modal wing for aerial-aquatic robotic vehicles. In *The Fourth IEEE RAS/EMBS International Conference on Biomedical Robotics and Biomechatronics*, pp. 681-687. Roma, Italy. doi:10.1109/iros.2010. 5650943

Lock, R. J., Vaidyanathan, R. and Burgess, S. C. (2013). Impact of marine locomotion constraints on a bio-inspired aerial-aquatic wing: experimental performance verification. *J. Mech. Robot.* **6**, 011001. doi:10.1115/1.4025471

Lovvorn, J. R. (2001). Upstroke thrust, drag effects, and stroke-glide cycles in wing-propelled swimming by birds. *Am. Zool.* **41**, 154-165. doi:10.1093/icb/41.2.154

Lovvorn, J. R., Jones, D. R. and Blake, R. W. (1991). Mechanics of underwater locomotion in diving ducks: drag, buoyancy and acceleration in a size gradient of species. *J. Exp. Biol.* **159**, 89-108.

Lovvorn, J. R., Croll, D. A. and Liggins, G. A. (1999). Mechanical versus physiological determinants of swimming speeds in diving Brünnich's guillemots. *J. Exp. Biol.* **202**, 1741-1752.

Lovvorn, J. R., Watanuki, Y., Kato, A., Naito, Y. and Liggins, G. A. (2004). Stroke patterns and regulation of swim speed and energy cost in free-ranging Brünnich's guillemots. *J. Exp. Biol.* **207**, 4679-4695. doi:10.1242/jeb.01331

Martin, G. R. (2017). *The Sensory Ecology of Birds*. Oxford University Press.

Necker, R. (2007). Head-bobbing of walking birds. *J. Comp. Physiol. A Neuroethol. Sens. Neural Behav. Physiol.* **193**, 1177-1183. doi:10.1007/s00359-007-0281-3

Pennycuick, C. J. (1987). Flight of auks (Alcidae) and other northern seabirds compared with southern procellariiformes: ornithodolite observations. *J. Exp. Biol.* **128**, 335-347. doi:10.1016/0198-0254(87)90303-7

Pete, A. E., Kress, D., Dimitrov, M. A. and Lentink, D. (2015). The role of passive avian head stabilization in flapping flight. *J. R. Soc. Interface* **12**, 0508. doi:10. 1098/rsif.2015.0508

Ponganis, P. J. (2015). *Diving Physiology of Marine Mammals and Seabirds*. Cambridge University Press.

Raikow, R. J., Bicanovsky, L. and Bledsoe, A. (1988). Forelimb joint mobility and the evolution of wing-propelled diving in birds. *Auk* **105**, 446-451.

Rayner, J. M. V. (1988). Form and function in avian flight. In *Current Ornithology, Vol. 5* (ed. Richard F. Johnston), pp. 1-66. Boston, MA: Springer.

Rayner, J. M. V. (1995). Dynamics of the vortex wakes of flying and swimming vertebrates. In *Biological Fluid Dynamics* (ed. C. P. Ellington and T. J. Pedley). *Symp. Soc. Exp. Biol.* **49**, 131-155.

Reggiani, C., Potma, E. J., Bottinelli, R., Canepari, M., Pellegrino, M. A. and Stienen, G. J. M. (1997). Chemo-mechanical energy transduction in relation to myosin isoform composition in skeletal muscle fibres of the rat. *J. Physiol.* **502**, 449-460. doi:10.1111/j.1469-7793.1997.449bk.x

Richman, S. E. and Lovvorn, J. R. (2008). Costs of diving by wing and foot propulsion in a sea duck, the white-winged scoter. *J. Comp. Physiol. B Biochem. Syst. Environ. Physiol.* **178**, 321-332. doi:10.1007/s00360-007-0225-9

Ros, I. G. and Biewener, A. A. (2016). Optic flow stabilizes flight in ruby-throated hummingbirds. *J. Exp. Biol.* **219**, 2443-2448. doi:10.1242/jeb.128488

Ros, I. G. and Biewener, A. A. (2017). Pigeons (C. livia) follow their head during turning flight: Head stabilization underlies the visual control of flight. *Front. Neurosci.* **11**, 1-12. doi:10.3389/fnins.2017.00655

Sato, K., Naito, Y., Kato, A., Niizuma, Y., Watanuki, Y., Charrassin, J. B., Bost, C.-A., Handrich, Y. and Le Maho, Y. (2002). Buoyancy and maximal diving depth in penguins: do they control inhaling air volume? *J. Exp. Biol.* **205**, 1189-1197.

Sato, K., Shiomi, K., Marshall, G., Kooyman, G. L. and Ponganis, P. J. (2011). Stroke rates and diving air volumes of emperor penguins: implications for dive performance. *J. Exp. Biol.* **214**, 2854-2863. doi:10.1242/jeb.055723

Schmid, D., Grémillet, D. J. H. and Culik, B. M. (1995). Energetics of underwater swimming in the great cormorant (Phalacrocorax carbo sinensis). *Mar. Biol.* **123**, 875-881. doi:10.1007/BF00349133

Simpson, G. G. (1946). *Fossil Penguins*. Bulletin of the American Museum of Natural History.

Storer, R. (1960). Evolution in the diving birds. In *Proceedings of the XII International Ornithological Congress* (ed. G. Bergman, K. O. Donner and L. v. Haartman), pp. 694-707. Tilgmannin Kirjapaino.

Vermeij, G. J. and Dudley, R. (2000). Why are there so few evolutionary transitions between aquatic and terrestrial ecosystems? *Biol. J. Linn. Soc.* **70**, 541-554. doi:10.1111/j.1095-8312.2000.tb00216.x

Vogel, S. (1994). *Life in Moving Fluids*. Princeton University Press.

Walker, J. A. and Westneat, M. W. (2000). Mechanical performance of aquatic rowing and flying. *Proc. R. Soc. B Biol. Sci.* **267**, 1875-1881. doi:10.1098/rspb. 2000.1224

Walker, J. A. and Westneat, M. W. (2002). Kinematics, dynamics, and energetics of rowing and flapping propulsion in fishes. *Integr. Comp. Biol.* **42**, 1032-1043. doi:10.1093/icb/42.5.1032

Walsh, S. A., Iwaniuk, A. N., Knoll, M. A., Bourdon, E., Barrett, P. M., Milner, A. C., Nudds, R. L., Abel, R. L. and Sterpaio, P. D. (2013). Avian cerebellar floccular fossa is not a proxy for flying ability in birds. *PLoS ONE* **8**, e67176. doi:10.1371/journal.pone.0067176

Watanuki, Y. and Burger, A. E. (1999). Body mass and dive duration in alcids and penguins. *Can. J. Zool.* **77**, 1838-1842. doi:10.1139/z99-157

Watanuki, Y. and Sato, K. (2008). Dive angle, swim speed and wing stroke during shallow and deep dives in common murres and rhinoceros auklets. *Ornithol. Sci.* **7**, 15-28. doi:10.2326/1347-0558(2008)7[15:DASSAW]2.0.CO;2

Watanuki, Y., Niizuma, Y., Gabrielsen, G. W., Sato, K., Naito, Y., Geir, W. G., Sato, K., Naito, Y., Gabrielsen, G. W., Sato, K. et al. (2003). Stroke and glide of wing-propelled divers: deep diving seabirds adjust surge frequency to buoyancy change with depth. *Proc. R. Soc. B Biol. Sci.* **270**, 483-488. doi:10.1098/rspb. 2002.2252

Watanuki, Y., Wanless, S., Harris, M., Lovvorn, J. R., Miyazaki, M., Tanaka, H. and Sato, K. (2006). Swim speeds and stroke patterns in wing-propelled divers: a comparison among alcids and a penguin. *J. Exp. Biol.* **209**, 1217-1230. doi:10. 1242/jeb.02128

Williams, T. M. (1999). The evolution of cost efficient swimming in marine mammals: limits to energetic optimization. *Philos. Trans. R. Soc. London. Ser. B Biol. Sci.* **354**, 193-201. doi:10.1098/rstb.1999.0371

Wilson, R. P. (2003). Penguins predict their performance. *Mar. Ecol. Prog. Ser.* **249**, 305-310. doi:10.3354/meps249305

Wilson, U. W. and Manuwal, D. A. (1986). Breeding Biology of the Rhinoceros Auklet on Protection Island, Washington. *Condor* **88**, 143-155. (doi:10.2307/1368909)